2017

High-field electron transport in doped ZnO

L. Ardaravičius
Center for Physical Sciences & Technology

O. Kiprijanovič
Center for Physical Sciences & Technology

J. Liberis
Center for Physical Sciences & Technology

See next page for additional authors

Authors
L. Ardaravičius, O. Kiprijanovič, J. Liberis, M. Ramonas, E. Šermukšnis, A. Matulionis, M. Toporkov, V. Avrutin, Ü. Özgür, and H. Morkoç

High-field electron transport in doped ZnO

2017 Mater. Res. Express 4 066301

(http://iopscience.iop.org/2053-1591/4/6/066301)

Materials Research Express

PAPER

High-field electron transport in doped ZnO

RECEIVED
3 April 2017

REVISED
15 May 2017

ACCEPTED FOR PUBLICATION
19 May 2017

PUBLISHED
6 June 2017

L Ardaravičius[1,3], O Kiprijanovič[1], J Liberis[1], M Ramonas[1], E Šermukšnis[1], A Matulionis[1], M Toporkov[2], V Avrutin[2], Ü Özgür[2] and H Morkoç[2]

[1] Center for Physical Sciences and Technology, Saulėtekio 3, LT-10257 Vilnius, Lithuania
[2] Department of Electrical and Computer Engineering, Virginia Commonwealth University, Richmond, VA 23284, United States of America
[3] Author to whom any correspondence should be addressed

E-mail: linas.ardaravicius@ftmc.lt

Keywords: doped ZnO, electron density, high electric field, self-heating effect, electron drift velocity, threshold power, soft damage

Abstract

Current–voltage characteristics have been measured for ZnO:Ga and Zn:Sb epitaxial layers with electron densities ranging from 1.4×10^{17} cm^{-3} to 1.1×10^{20} cm^{-3}. Two-terminal samples with coplanar electrodes demonstrate virtually ohmic behavior until thermal effects come into play. Soft damage of the samples takes place at high currents. The threshold power (per electron) for the damage is nearly inversely proportional to the electron density over a wide range of electron densities. Pulsed voltage is applied in order to minimize the thermal effects, and thus an average electric field of 150 kV cm^{-1} is reached in some samples subjected to 2 ns voltage pulses. The results are treated in terms of electron drift velocity estimated from the data on current and electron density under the assumption of uniform electric field. The highest velocity of $\sim 1.5 \times 10^{7}$ cm s^{-1} is found at an electric field of $\sim$100 kV cm^{-1} for the sample with an electron density of 1.4×10^{17} cm^{-3}. The non-ohmic behavior due to hot-electron effects is weak, and the dependence of the electron drift velocity on the doping resembles the variation of mobility.

1. Introduction

Semiconducting zinc oxide (ZnO) attracts considerable attention for a variety of electronic and optoelectronic applications, including transparent field-effect transistors for flat-screen displays, photodetectors, transparent electrodes, etc [1–3]. The epitaxial technology is inexpensive, albeit is not sufficiently well developed yet. Favorable conditions for electron transport at high electric fields and expected improvement in structural quality of ZnO epitaxial structures make this material attractive for high speed/power transistors operating at centimeter and millimeter-wave frequencies [4].

At room temperature, the electron transport in heavily doped ZnO is mainly controlled by scattering on ionized impurities and extended defects, while polar scattering by longitudinal optical phonons (LO phonons) is important at low and moderate electron densities [5, 6]. The electron mobility exceeding 400 cm^2(Vs)$^{-1}$ has been achieved at room temperature in ZnO epitaxial layers with low residual impurity density [7].

Data on high-field electron transport in epitaxial ZnO are scarce [8]. An electron drift velocity of 7.6×10^{6} cm s^{-1} has been reported for nominally undoped ZnO at room temperature for an applied electric field of 94 kV cm^{-1} [9]. Hot-electron and hot-phonon effects should be taken into consideration for doped channels: a non-monotonous dependence of the hot-electron energy relaxation on the electron density has been observed experimentally and explained with the aid of Monte Carlo modeling [10]. The results of Monte Carlo simulations of electron transport in ZnO are available in a number of papers [4, 11–13]. However, to the best of our knowledge, no experimental study of doping-dependent electron drift velocity has been published up to date.

In this study, the current–voltage characteristics were measured for Ga- and Sb-doped ZnO films in a wide range of electric fields and electron densities. The thermal effects were minimized by employing the pulsed voltage technique. The electron drift velocity was deduced assuming uniform electric field and constant electron density.

Table 1. Electron density, Hall mobility, and channel thickness for the ZnO films at room temperature.

Wafer	Dopant	n cm^{-3}	μ cm^2 Vs^{-1}	d nm
#567	Ga	1.4×10^{17}	106	330–340
#570	Ga	5.5×10^{17}	73	350
#639	Ga	4.9×10^{18}	23	300
#753	Ga	1×10^{19}	57	200
#751	Ga	1.1×10^{19}	66	200
#661	Ga	1.7×10^{19}	25–30	150
#487	Sb	4.6×10^{19}	110	170
#658	Ga	1.1×10^{20}	48	350

2. Samples

The ZnO films were grown on a-plane sapphire substrates by plasma-enhanced molecular beam epitaxy (PE-MBE). RF plasma cell operating at 400 W was employed as a source of reactive oxygen, and the Knudsen cells were used to evaporate Zn, Ga, and Sb. The growth was monitored *in situ* by reflection high-energy electron diffraction (RHEED). To pave the way for the initiation of two-dimensional growth, a 15 nm-thick low-temperature ZnO buffer layer was deposited at 300 °C followed by annealing at 700 °C prior to the growth of doped ZnO layers at 600 °C. The layer thicknesses were 150–350 nm. Structural properties and surface morphology of the layers were studied by x-ray diffraction, transmission electron microscopy, and atomic force microscopy. The growth conditions, the structure, and the electrical properties at low fields are similar to those reported for doped ZnO layers [6, 10, 14].

The Hall effect measurements were performed in van der Pauw configuration with soldered indium contacts. The electron density, mobility, and the channel thickness d are listed in table 1. The Hall mobility μ values range from 106 cm^2 (V · s)$^{-1}$ to 23 cm^2 (V · s)$^{-1}$ in the investigated samples with the corresponding electron density n varying from 1.4×10^{17} cm^{-3} to 1.1×10^{20} cm^{-3}.

The transmission line model (TLM)patterns were processed with evaporated stacks of Ti/Au (25 nm/50 nm) acting as coplanar ohmic contacts. The channel width w was 250–300 μm and the channel lengths (inter-electrode distance) L were 1.7, 2.9, 3.9, 5.8, 6.1, 6.9, 9.2, 9.9, 14.8, 16,8, 17.3 μm. The contact resistance R_c was estimated at low electric fields from the dependence of the sample resistance on the channel length.

3. Methods

The electron transport measurements were carried out at high electric fields on two-electrode samples chosen from the TLM structures. The semi-automated nanosecond-pulsed voltage technique was used to investigate current–voltage (I–V) characteristics [15–17]. The sample was placed into a gap of a micro-strip line. The few-nanosecond pulses enabled the minimization the channel self-heating due to the current [15]. The electron drift velocity was estimated assuming that the electric field E was uniform and the electron density was independent of the electric field: $v_{dr} = I/(\mathrm{enwd})$, where e is the elementary charge.

The channels suffered from soft damage at high electric fields. The damage was characterized by the increase in the low-field channel resistance measured before and after the high-field experiment. We present the results up to a damage level not exceeding 5%. The soft damage turned into the channel breakdown at higher currents.

Ensemble Monte Carlo simulations were carried out for bulk wurtzite ZnO crystals at a fixed lattice temperature. The electron motion in uniform electric field and scattering in one-valley spherical parabolic conduction band were considered within the known model [12]. The following scattering mechanisms were included in the simulations: acoustic phonon scattering, LO phonon scattering, and elastic ionized impurity scattering.

The total scattering rate as a function of electron energy is illustrated in figure 1 (black line) together with the partial rates for two dominant mechanisms: LO phonon and ionized impurity scattering (red and blue lines). The impurities were treated as electron-screened non-interacting point charges, any impurity clustering and impurity vibration modes were ignored. The electron scattering into the upper valleys was expected to be insignificant, and the inter-valley transfer was neglected for the electric fields under investigation. The results of the Monte Carlo simulation are used to calculate the electron distribution function, the electron drift velocity, and the electron energy.

4. Results and discussion

The applied electric field heats the electrons in doped ZnO as demonstrated through the noise measurements [10]. Simultaneously, the electron drift velocity increases with the field.

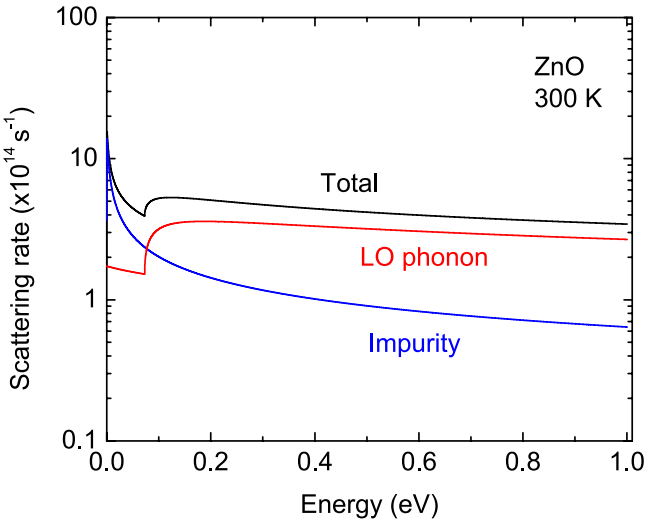

Figure 1. Dependence of scattering rates on electron kinetic energy for ZnO at an electron density of 1.4×10^{17} cm^{-3} and ionized impurity density of 1.1×10^{18} cm^{-3}.

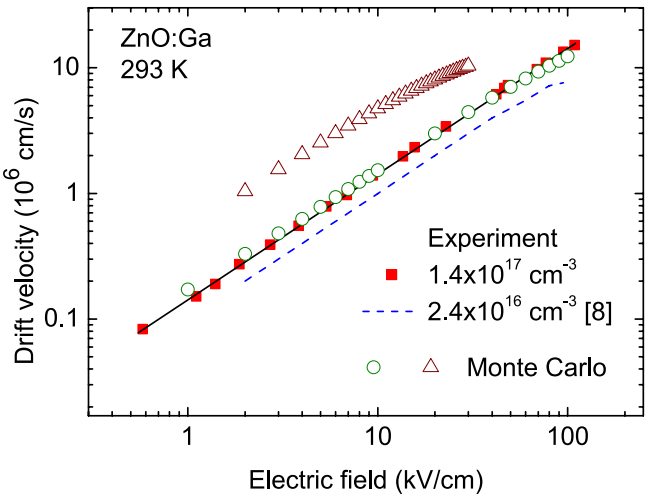

Figure 2. Dependence of drift velocity on applied electric field for ZnO sample #567 (closed squares). Voltage pulse duration is 2 ns. Dashed blue line: experiment with 300 ns voltage pulses for nominally undoped sample with electron density of 2.4×10^{16} cm^{-3} [8]. Monte Carlo simulations: triangles—no impurities, circles—electron density of 1.4×10^{17} cm^{-3} and ionized impurity density of 1.1×10^{18} cm^{-3}. Solid line stands for $v_{dr} \propto E$.

The experimental data on the electron drift velocity for sample #567 are illustrated in figure 2 (red squares). The highest value for the drift velocity of $\sim 1.5 \times 10^7$ cm s^{-1} is obtained at a field of 108 kV cm^{-1}. This velocity value exceeds the published experimental value of $\sim 7.6 \times 10^6$ cm s^{-1} at approximately 100 kV cm^{-1} measured in MBE-grown, nominally undoped ZnO layers with electron density of $\sim 2.4 \times 10^{16}$ cm^{-3} (figure 2, dashed blue line, [8]).

Triangles in figure 2 illustrate the results of Monte Carlo simulations for nominally undoped ZnO within the framework of the model [10]. The non-ohmic behaviour due to hot electrons is resolved at electric field below 30 kV cm^{-1} (triangles). A comparison of the triangles with the experimental data reveals an essential discrepancy: the simulated drift velocity (triangles) substantially exceeds the experimental values. A simple explanation is neglected impurity scattering. The experimental data (figure 2, squares) can be fitted reasonably well (circles) if the impurity scattering rate given by the blue line in figure 1 is used. The blue line assumes that the standard ionized impurity scattering is enhanced, as if the impurity density exceeded the electron density. The enhancement of the elastic impurity scattering can originate from different routes. As an example, suppose that the impurity atoms form clusters. For the same impurity density, the number of scattering centers is reduced due to the clustering, but the scattering cross section of one cluster increases in proportion to the squared number of atoms in the cluster. As a result, the scattering rate increases. Alternatively, one could also assume that some donors were compensated by acceptors; thus the electron density would be assumed lower than the total density of ionized donors and acceptors. Moreover, complexes with native defects could form. The extended and complex defects were not treated in detail.

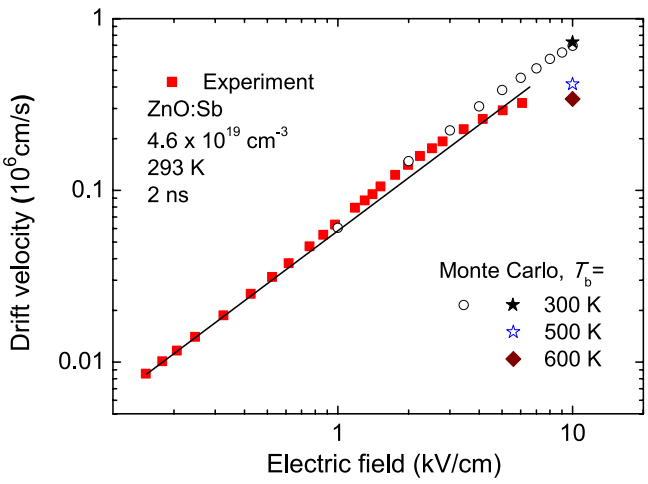

Figure 3. Dependence of drift velocity on applied electric field for ZnO sample #487 (closed squares) [15]. Voltage pulse duration is 2 ns. Line stands for the Ohm's law. Monte Carlo simulation for hot-phonon lifetime of 1 ps at background temperatures: 300 K (open circles and closed black star), 500 K (open blue star), and 600 K (diamond).

The fitting of the experimental data was achieved when a fitting factor was used to increase artificially the impurity scattering rate over the rate when the density of ionized impurities equaled the density of electrons.

The electric field $E \sim 100\,\mathrm{kV\,cm^{-1}}$ was found to be strong enough to heat the electrons in doped ZnO [10]. On the other hand, the Ohm's law approximately holds: the red squares are close to the black line in figure 2. This indicates that the hot electrons cause a weak if any non-ohmic behavior at electric fields up to $100\,\mathrm{kV\,cm^{-1}}$ in this particular sample. Consequently, the traditional way of extracting additional information on hot electrons from the non-ohmic behavior of the electron drift velocity fails for doped ZnO.

The employment of 2 ns voltage pulses enabled the I–V measurements at electric fields up to $150\,\mathrm{kV\,cm^{-1}}$ for sample #570 ($n = 5.5 \times 10^{17}\ \mathrm{cm^{-3}}$; $\mu = 73\ \mathrm{cm^2\,Vs^{-1}}$).

Short voltage pulses help to reduce the thermal walkout effect unless the electron density is high and the electric field is strong. Figure 3 presents the experimental results at a high electron density of $4.6 \times 10^{19}\,\mathrm{cm^{-3}}$ (sample #487) for electric fields below $6\,\mathrm{kV\,cm^{-1}}$ (red squares) [15]. As the electric field increases from $0.7\,\mathrm{kV\,cm^{-1}}$ to $3\,\mathrm{kV\,cm^{-1}}$, the non-ohmic behavior with the super-linear drift velocity-field characteristic is clearly evident. A weak super-linear dependence is also obtained through Monte Carlo simulation at $E < 3\,\mathrm{kV\,cm^{-1}}$ under assumption of constant background temperature of 300 K (open circles). This can be attributed to the elastic impurity scattering which is the dominant scattering mechanism at this electron density.

As the electric field is increased further and exceeds $\sim 3\,\mathrm{kV\,cm^{-1}}$, the experimental drift velocity exhibits a sub-linear non-ohmic behavior (closed squares) attributed to thermal walkout (sample self-heating). Under these conditions, only a weak sub-linearity is obtained from the Monte Carlo simulation if the background temperature is kept constant (figure 3, open circles). An essentially stronger deviation is obtained if the simulation is carried out for the enhanced background temperature at a field of $10\,\mathrm{kV\,cm^{-1}}$ as illustrated in figure 3 (open star and diamond). According to the simulation, the drift velocity decreases as the background temperature increases.

The thermal walkout turns into the electrothermal breakdown at stronger electric fields even when the voltage pulses of 2 ns are applied. The alternative interpretation of the sub-linear experimental dependence in terms of hot-phonon lifetime requires unrealistically long lifetimes—significantly longer than 1 ps—if the thermal walkout is ignored.

The manifestation of the thermal walkout is illustrated in figure 4. The experimental dependence of the drift velocity on the supplied power per electron, $P_e = ev_{\mathrm{dr}}E$ demonstrates an almost square-root dependence, $v_{\mathrm{dr}} \propto \sqrt{P_e}$ (figure 4, solid line) in agreement with the virtually linear current–voltage characteristics at low and moderate electric fields (figure 2). The more noticeable deviations from the Ohm's law are observed for high fields in the samples with high electron density. It should be noted that the measurements were terminated when the soft damage of the sample was noticed. The threshold power per electron, P_{th}, for soft damage gradually decreases as the electron density increases (figure 5, squares). A nearly inverse proportionality holds in the density range from 5.5×10^{17} $\mathrm{cm^{-3}}$ to $1.1 \times 10^{20}\,\mathrm{cm^{-3}}$ (figure 5, squares) while the threshold power P_{th} ranges from $2.2 \times 10^{-7}\,\mathrm{W/electron}$ to $1.4 \times 10^{-9}\,\mathrm{W/electron}$, correspondingly. The proportionality indicates that the product of the threshold power for the soft damage and the electron density, $P_{\mathrm{th}}n$, demonstrates a weak if any dependence on the electron density n (figure 5, crosses). In other words, the supplied power per unit volume rather than the power per electron governs the soft damage in the samples with varying electron densities. This behavior suggests that the observed channel damage is caused by the elevated sample background temperature, despite the pulsed measurements (the sample

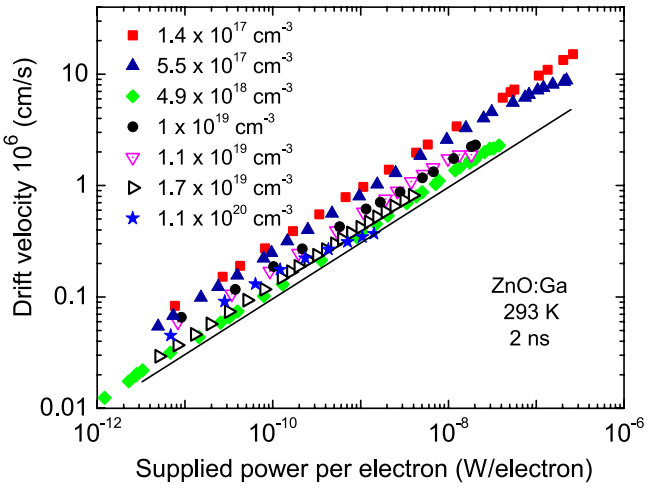

Figure 4. Experimental dependence of hot-electron drift velocity on the supplied power per electron for doped ZnO at various electron densities. Voltage pulse duration is 2 ns. Solid line stands for $v_{dr} \propto \sqrt{P_e}$.

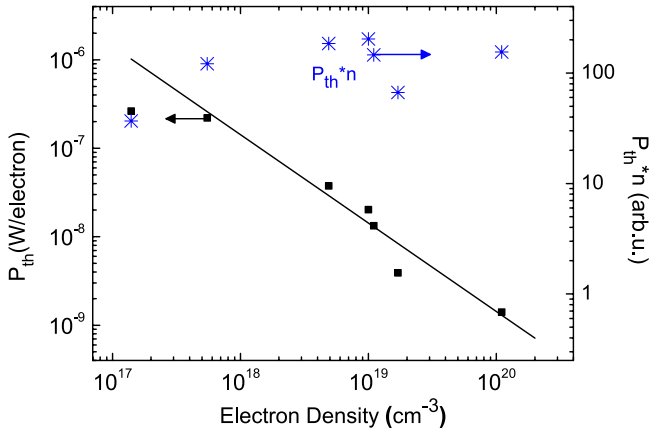

Figure 5. Threshold power for soft damage in doped ZnO versus electron density: the power per electron, P_{th} (black squares), and the power per unit volume, $P_{th}n$ (blue crosses). Voltage pulse duration is 2 ns.

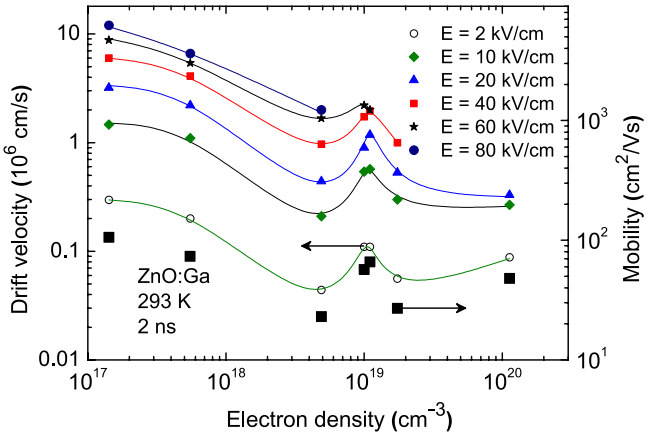

Figure 6. Experimental dependence of hot-electron drift velocity and Hall mobility (squares) on electron density for various fixed electric fields in doped ZnO. Lines guide the eye. Data at high fields for high-density channels are missing because of soft damage. Voltage pulse duration is 2 ns.

self-heating rather than the hot-electron effect). The same holds for the preceding non-ohmic transport at high electric fields as demonstrated through the comparison of experimental data and Monte Carlo simulations [15].

The electron drift velocity as a function of electron density is shown in figure 6 for various ZnO samples under constant applied electric field. As indicated, an application of short voltage pulses allows one to exclude the

thermal walkout for low and moderate electric fields [15]. As a result, the density dependence of the drift velocity at the electric field of 2 kV cm^{-1} (circles), 10 kV cm^{-1} (diamonds), and 20 kV cm^{-1} (triangles) resembles that of the drift mobility (figure 6, squares), i.e. the electron velocity is governed by drift mobility up to electric field of ~60 kV cm^{-1}. In agreement with the mobility data, the local peak of velocity forms at $\sim 1 \times 10^{19}$ cm^{-3}. Because of the sample damage, the peak is not resolved at an electric field of 80 kV cm^{-1} (closed circles).

It is worth noting that the magnitude of the local peak in figure 6 does not increase as the electric field is changed. Therefore, the origin of the peak cannot be associated with hot electrons and hot phonons in contrast to the plausible explanation in terms of the resonance decay of hot phonons as in GaN-based two-dimensional electron gas channels [18]. In the GaN case, the resonance enhances as the electric field increases and can be associated with ultrafast decay of hot phonons. However, no improvement of the resonance is observed at higher electric fields in the investigated three-dimensional ZnO (figure 6). The microwave noise measurements demonstrate the local minimum of the hot-electron energy relaxation time in the same samples of doped ZnO at electron density of $\sim 1.4 \times 10^{19}$ cm^{-3} [10]; the result is interpreted in terms of the resonance decay of hot phonons.

5. Conclusions

Nanosecond pulsed voltage measurements were carried out for epitaxial ZnO layers doped with gallium and antimony. The experiments yielded the hot-electron drift velocity in the wide range of the electron densities. The results were fitted with those of the Monte Carlo simulation when the elastic impurity scattering rate was assumed to exceed substantially the rate expected from single-charged impurities. The Ohm's law approximately held in the electric field range up to 100 kV cm^{-1} at an electron density of 1.4×10^{17} cm^{-3}, but the range shrunk at higher electron densities. The maximum drift velocity of $\sim 1.5 \times 10^{7}$ cm s^{-1} was measured at 108 kV cm^{-1} field. The non-ohmic behavior at high fields preceded the sample damage. The threshold power per electron for the soft damage was found inversely proportional to the electron density, and the damage was associated with the thermal walkout (an increase in the background temperature). The local peak of the electron drift velocity was found at around 1×10^{19} cm^{-3}; in correlation with that in the mobility deduced from the Hall effect measurements. No correlation of the peak with the hot-electron behavior was found.

Acknowledgment

This research is funded by the Research Council of Lithuania (grant No. APP-5/2016). At Virginia Commonwealth University, this work is supported by Air Force Office of Scientific Research (AFOSR) under Grant FA9550-12-1-0094.

References

[1] Morkoç H and Özgür Ü 2009 *Zinc Oxide: Fundamentals, Materials and Device Technology* (Weinheim: Wiley)
[2] Klingshirn C, Fallert J, Zhou H, Sartor J, Thiele C, Maier-Flaig F, Schneider D and Kalt H 2010 *Phys. Status Solidi* B **247** 1424
[3] Liu H, Avrutin V, Izyumskaya N, Özgür Ü, Morkoç H 2010 *Supperlattices Microstruct.* **48** 458
[4] O'Leary S K, Foutz B E, Shur M S and Eastman L F 2010 *Solid State Commun.* **150** 2182
[5] Look D C, Leedy K D, Tomich D H and Bayraktaroglu B 2006 *Appl. Phys. Lett.* **96** 062102
[6] Liu H Y, Avrutin V, Izyumskaya N, Özgür Ü, Yankovich A B, Kvit A V, Voyles P M and Morkoç H 2012 *J. Appl. Phys.* **111** 103713
[7] Tsukazaki A, Ohtomo A and Kawasaki M 2006 *Appl. Phys. Lett.* **88** 152106
[8] Sasa S, Hayafuji T, Kawasaki M, Nakashima A, Koike K, Yano M and Inoue M 2008 *Phys. Status Solidi* C **5** 115
[9] Sasa S, Maitani T, Furuya Y, Amano T, Koike K, Yano M and Inoue M 2011 *Phys. Status Solidi* A **208** 449
[10] Šermukšnis E, Liberis J, Ramonas M, Matulionis A, Toporkov M, Liu H Y, Avrutin V, Özgür Ü and Morkoç H 2015 *J. Appl. Phys.* **117** 065704
[11] Albrecht J D, Ruden P P, Limpijumnong S, Lambrecht W R L and Brennan K F 1999 *J. Appl. Phys.* **86** 6864
[12] Furno E, Bertazzi F, Goano M, Ghione G and Bellotti E 2008 *Solid-State Electron.* **52** 1796
[13] Hadi W A, Shur M S and O'Leary S K 2012 *J. Appl. Phys.* **112** 033720
[14] Liu H Y, Izyumskaya N, Avrutin V, Özgür Ü, Yankovich A B, Kvit A V, Voyles P M and Morkoç H 2012 *J. Appl. Phys.* **112** 033706
[15] Ardaravičius L, Kiprijanovič O, Liberis J, Ramonas M, Šermukšnis E, Matulionis A, Toporkov M, Avrutin V, Özgür Ü and Morkoç H 2016 arXiv:1605.09117
[16] Ardaravičius L, Ramonas M, Liberis J, Kiprijanovič O, Matulionis A, Xie J, Wu M, Leach J H and Morkoç H 2009 *J. Appl. Phys.* **106** 073708
[17] Ardaravičius L, Kiprijanovič O, Liberis J, Matulionis A, Šermukšnis E, Ferreyra R A, Avrutin V, Özgür Ü and Morkoç H 2015 *Semicond. Sci. Technol.* **30** 105016
[18] Ardaravičius L, Liberis J, Kiprijanovič O, Matulionis A, Wu M and Morkoç H 2011 *Phys. Status Solidi* **5** 65